

Vibrations of roll swage jointed plates

Mauro Caresta (1), David Wassink (2)

(1) School of Mechanical and Manufacturing Engineering, University of New South Wales, Sydney, NSW 2052, Australia

(2) Australian Nuclear Science and Technology Organisation (ANSTO), Lucas Heights, NSW 2234, Australia

PACS: 43.40.At; 43.40.Dx

ABSTRACT

The aim of this work is to model the vibrational behaviour of thin plates joined to a stiff orthogonal side plate using the technique of 'roll swaging'. Swage joints are typically found in plate-type fuel assemblies for nuclear reactors. Since they are potentially liable to flow-induced vibrations, it is crucial to be able to predict their dynamic characteristics. It is shown that the contact between the plates resulting from the swage can be modelled assuming a perfect clamp of all the degrees of freedom but the rotational around the axis parallel to the swage. A modal analysis was performed on different specimens and the values of the first natural frequencies are used to find the equivalent torsional spring stiffness, by matching these frequencies with the results obtained from a finite element model (FEM).

INTRODUCTION

Plate-type fuel assemblies are used in several research reactors where a high neutron flux is desired. A plate-type assembly consists of several thin plates containing a uranium mixture, clad with aluminium and mounted in a box-type assembly. They are potentially affected by structural instabilities due to the interaction with the coolant flow [1-3]. Miller [4] used the wide beam theory to investigate the static instability of the plates. Other researchers modelled the plates using the thin plate theory assuming simply-supported boundary conditions [5] or fully-clamped edges [6]. Kim and Davis [7] improved the previous works assuming plates as laterally fixed but elastically restrained in rotation. The aim of this work is to give a theoretical and experimental justification of the model used in Ref. [7]. In a typical fuel assembly the plates are inserted into slots machined into the side walls of the fuel box. The clamping of the plates to the box is generally assured by a swage between adjacent plates. The swage is obtained by forcing a swage cutting wheel into the aluminium ridge between the slots. The shape of the cutting edge results in plastic deformation of the area surrounding the swage, and presses the material onto the plate, creating the clamp as shown in Figure 1.

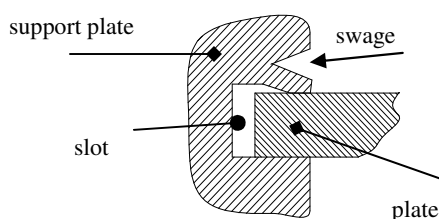


Figure 1. Schematic diagram of a typical swage joint.

The nature of the clamping is crucial to predict the vibrational behaviour of a fuel assembly. A perfect clamp completely constrains all six degrees of freedom at the edges of the fuel plates. In this work it is suggested that the swaging process results in a clamp that fixes all the degrees of freedom but the rotational around the axis parallel to the swage. For small rotations, as assumed by the linear vibrations theory, the effect of the swage joint is shown to be a torsional spring whose stiffness is related to the quality of the swage. A good swage leads to a very high stiffness that approaches the ideal case of a perfect clamp, while a poor swage is likely to result in a lower stiffness value tending to the case of a simple support. The model used in this work is built according to the data of some specimens that were made at the Australian Nuclear Science and Technology Organisation (ANSTO) in order to show that the changing of some parameters in the swaging process results in a shift of the natural frequencies. The aim of this work is to present a theoretical explanation of the abovementioned experimental evidence. The specimens, shown in Figure 2, were tested by clamping the bottom of the support in a vice and performing an impact hammer test to detect the natural frequencies by inspection of the Frequency Response Function (FRF). A laser vibrometer was used to measure the response close to the corner of the plate to maximise the visibility of all the modes.

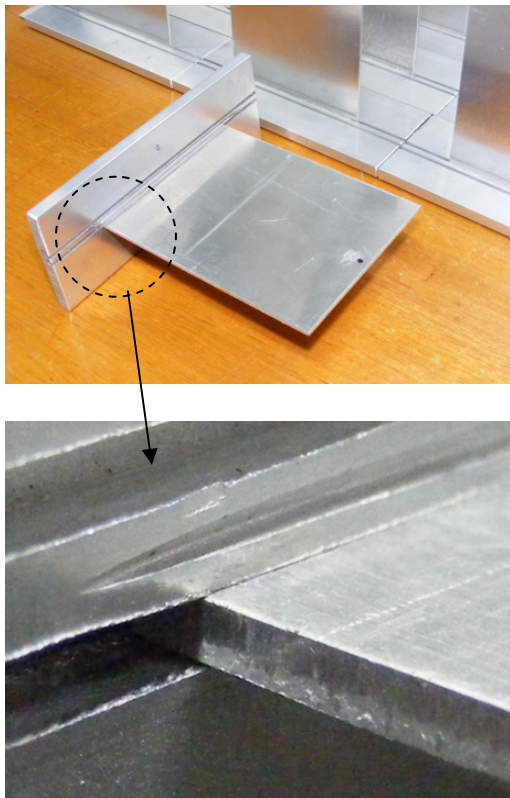


Figure 2. A specimen used for the modal analysis tests.

SWAGING PROCESS SIMULATION

To understand the nature of the contact between the plate and the support, a simple two dimensional model is created to simulate the swaging process. It is solved using Nastran Implicit Non-Linear (Solver 600) [8]. The swage wheel is modelled as a rigid wedge and is moved toward the support. The material is Aluminium with density $\rho = 2700 \text{ Kg m}^{-3}$, Youngs modulus $E = 69 \text{ MPa}$, Poisson ratio $\nu = 0.33$ and perfect plastic behaviour with Yield stress of 280 MPa . A more precise stress-strain curve should be used in order to improve the results. Figure 3 shows the deformation from the simulation. It can be seen that the deformed material presses the top of the plate to create the swage clamp. The different colours are related to the Von Mises stress.

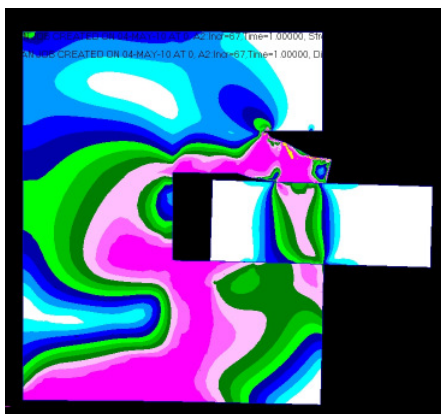


Figure 3. Swaging process simulation with Nastran.

DYNAMIC BEHAVIOUR OF THE SWAGE

Inspecting the results from the swaging simulation, a scheme is reproduced in Figure 4 to study the kinematics of the joint. It is reasonable to assume that after the swage is completed the plate can not translate along the y and z directions and it can not rotate around the y axis. In theory a translation in x direction and a rotation around z are also possible but it would not affect the dynamics of the plate in bending vibrations. Only the in plane motion will be altered, but this happens at much higher frequency and is therefore considered constrained in this work. A small rotation θ in x direction is possible around the contact line passing by point C_0 allowing a compression along the contact line L , as shown in Figure 4.

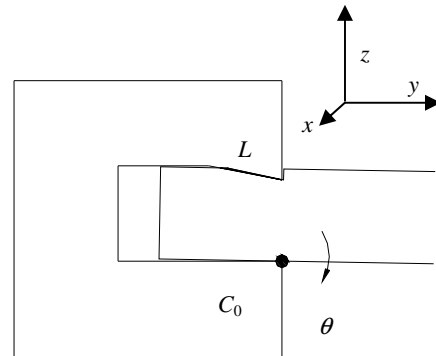


Figure 4. Small rotation of the plate in the swage joint

Considering a small clockwise rotation θ around the point C_0 , the component of the displacement normal to the contact line, which coordinate is $\xi_i \in [0, L]$, results in the compression of the material and then in a reaction force per unit rotation given by

$$df_i = \varepsilon E (dA) r_i \cos \delta, \quad dA = w (d\xi) \quad (1)$$

where ε is the strain, A and w are the area and width of the contact respectively. Other parameters arise from the geometry of the swage and are given by

$$r_i = \xi_i^2 + r_0^2 - 2\xi_i r_0 \cos \gamma, \quad \gamma = \frac{\pi}{2} + \varepsilon, \quad \varepsilon = \tan^{-1}(h_s / d_s) \quad (2)$$

$$\delta_i = \cos^{-1} \left(\frac{r_N^2 - r_0^2 + \xi_i^2}{2r_N l} \right) \quad (3)$$

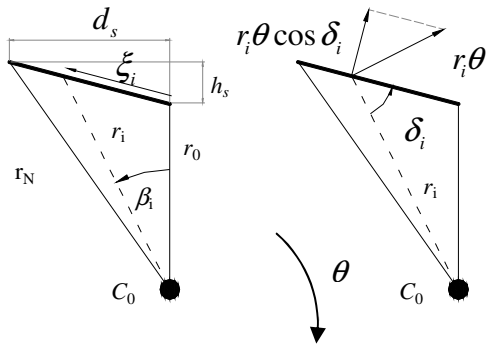


Figure 5. Kinematics of the swage joint.

All the forces normal to the contact line are equivalent to a force of magnitude

$$F_s = \int_{\xi=0}^{\xi=L} df_i \tag{4}$$

and with a lever arm b respect to point C_0 given by $b = H_b \sin \epsilon + 2/3L$. H_b is the height of the plate from point C_0 to point C_0 shown in Figure 6. The global effect is then a moment to point C_0 given by $M_s = F_s \theta b$ that can be rewritten as

$$M_s = K_s \theta, \quad K_s = F_s b \tag{5}$$

K_s is the equivalent torsional spring of the swage joint. The exact value has to be found by matching experimental and FEM results for the first natural frequency.

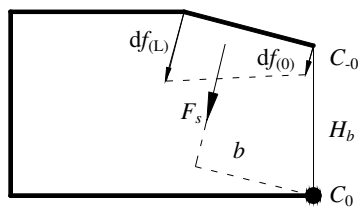


Figure 6. Force resultant from a small rotation of the plate.

A similar model can be used to calculate the reaction moment when the plate is rotating anticlockwise. In this case the plate is likely to rotate around the point C_0 . The moment is likely to have a different value leading to a non-linear spring characteristic, with different stiffness for the positive and negative rotations.

FEM MODEL OF THE JOINED PLATES

An FEM model is built according to the dimension of the specimens. The plate and the support are meshed using QUADR plate elements. The support is clamped at the base to simulate the clamping of the real model to a vice. The plate is connected to the support using bush elements with adjustable torsional spring around the x axis. The first five mode shapes are reported in Figure 7 for a perfect clamp situation.

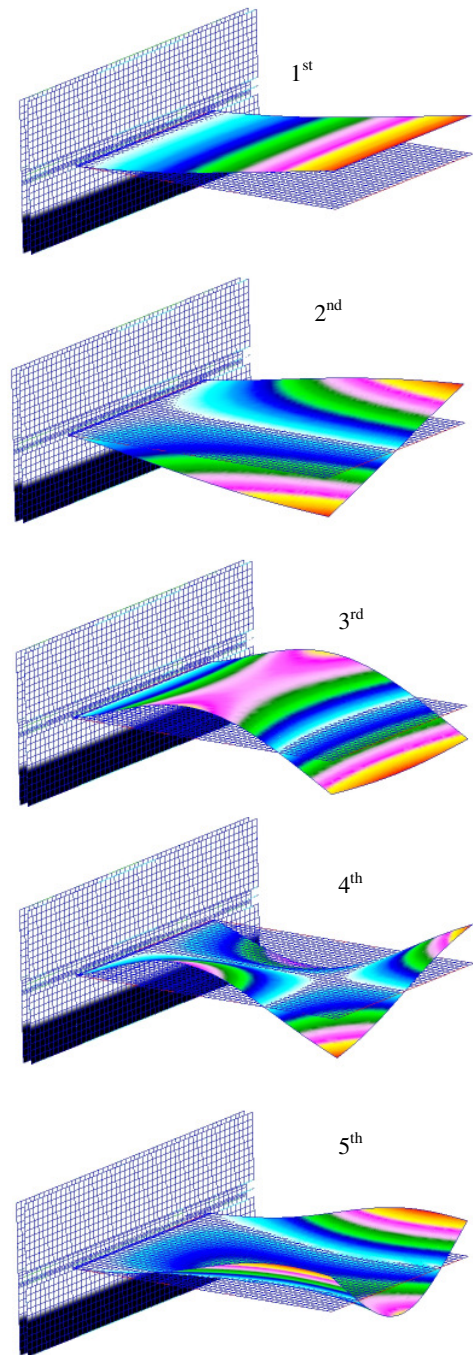


Figure 7. The first five mode shapes for a perfect clamped plate.

In the case where a simple support was used, the first mode degenerated into a rigid body rotation (0 Hz) around the swage axis. The other mode shapes were practically the same except for a slightly bigger rotation at the connection with the support. Different values for the torsional spring were used to simulate the conditions between a perfect clamp ($K_s \rightarrow \infty$) and a simple support ($K_s = 0$). The first five natural frequencies are normalised with respect to the perfect clamp case and are plotted versus the spring stiffness in Figure 8. Convergence to the perfect clamp case is achieved for a value of around $K_s = 200$ Nm/rad. Observing the slope of the curves it can be seen that the sensitivity first increases, reaching a maximum at 10 Nm/rad for the first natural frequency, and at 100 Nm/rad for the fifth natural frequency. The slope decreases again approaching the ideal clamped case. The lower order modes are more affected by the spring stiffness.

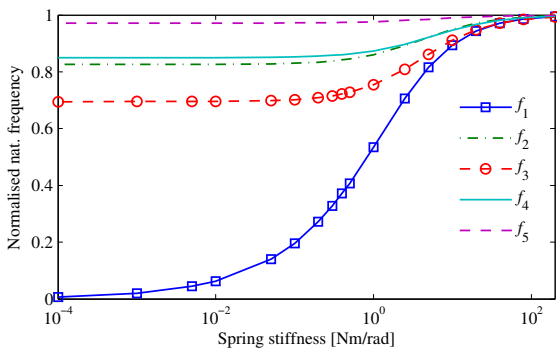


Figure 8. Variation of the natural frequencies with the spring stiffness (FEM results).

Figure 9 shows the same data as in the previous figure but arranged with respect to the natural frequency order. A characteristic stepwise variation between the two extreme situations of perfect clamp and simple support is observed. The presented arrangement of the results is useful to compare the frequencies with the experimental results.

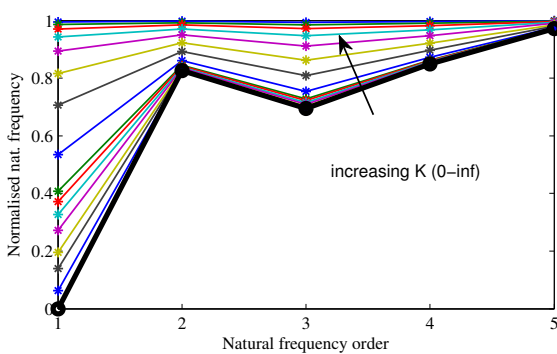


Figure 9. Normalised first five natural frequencies (FEM results).

Figure 10 shows the first natural frequencies of some specimens obtained by setting the roll swaging wheel at different heights with respect to the plates. It can be seen that the trend of the curves is similar to the FEM results presented in Figure 9.

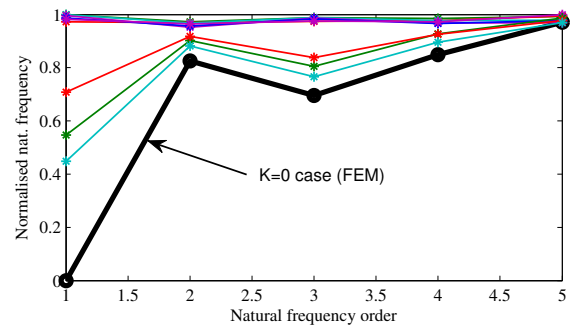


Figure 10. Normalised first five natural frequencies (experimental results).

Figure 11 shows the results updating the value of the torsional spring in the FE model to match the first natural frequency of two experimental results. The maximum error for the other frequencies is around 3%. A better estimation of the spring stiffness would need an update considering the global effect on more resonances in a desiderate frequency range.

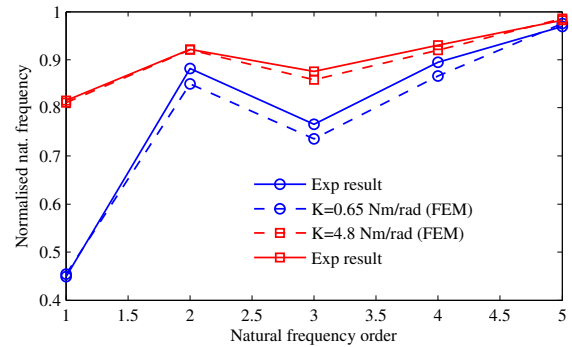


Figure 11. Matching of the natural frequencies by FEM updating.

CONCLUSIONS

The work presented shows a first step to model the dynamic behaviour of swage joints and open a variety of issues that need to be studied in more depth. In particular a more precise model of the swaging process using the non-linear capabilities of FE modelling is required. A more sophisticated FEM updating process able to match the results of more natural frequencies will give an improved value for the equivalent torsional spring. In order to validate the results it is also necessary to set up a consistent method of swaging the specimens with the aim of finding the sensitivity of the natural frequencies to parameters such as height and depth (applied force) of the swage and the cutting profile of the, swage wheel. The results can be then used to validate the swaging simulations from FEM. From a reliable FE model it may be possible to figure out the equivalent torsional spring stiffness without requiring an updating of the linear model with the experimental results. A non linear behaviour is also evident from the Frequency Response Functions of some specimens, by the leaning forward of some resonance peaks. The reason could be the asymmetry of the torsional moment as discussed before or a hardening effect as given by cubic stiffness as in Duffing oscillator [9]. The more plausible explanation is another matter worthy of further exploration.

REFERENCES

- ¹ R. D. Blevins, "Flow-induced vibration in nuclear reactors: a review", *Progress in Nuclear Energy*, **4**, 25-49 (1979)
- ² M. P. Paidoussis, in *Practical Experiences with Flow-Induced Vibrations*, Vol. 829-832 (Ed: E. E. Naudascher and D. Rockwell), Springer-Verlag, Berlin 1980.
- ³ M. Ho, G. Hong and A. N. F. Mack, Experimental investigation of flow-induced vibration in a parallel plate reactor fuel assembly, *15th Australasian Fluid Mechanics Conference*, Sydney, Australia, 13-17 December 2004
- ⁴ D. R. Miller, "Critical flow velocities for collapse of reactor parallel-plate fuel assemblies", *Journal of Engineering for Power-Transactions of the ASME*, **82**, 83-95 (1960)
- ⁵ S. J. Pavone and H. A. Scarton, "Laminar flow-induced deflections of stacked plates", *Nuclear Engineering and Design*, **74**, 79-89 (1982)
- ⁶ D. C. Davis and H. A. Scarton, "Flow-induced plastic collapse of stacked fuel plates", *Nuclear Engineering and Design*, **85**, 193-200 (1985)
- ⁷ G. Kim and D. C. Davis, "Hydrodynamic instabilities in flat-plate-type fuel assemblies", *Nuclear Engineering and Design*, **158**, 1-17 (1995)
- ⁸ *MSC Nastran Implicit Nonlinear (SOL 600) User's Guide*, 2007.
- ⁹ S. S. Rao, *Mechanical Vibrations*, Prentice Hall, 4th Edition, Singapore, 2005.